International Journal of Steel Structures (2020) 20(2):464–479
https://doi.org/10.1007/s13296-019-00297-1

Online ISSN 2093-6311
Print ISSN 1598-2351

Offshore Triceratops Under Impact Forces in Ultra Deep Arctic Waters

Srinivasan Chandrasekaran[1] · **R. Nagavinothini**[1]

Received: 10 June 2019 / Accepted: 1 November 2019 / Published online: 5 November 2019

Abstract
In the recent years, offshore oil drilling and production is moving towards ultra-deep Arctic region which demands an adaptable structural form. Apart from the environmental loads, offshore structures in Arctic region will also be subjected to impact forces arising due to ship platform collision. Such loads may endanger the safety of the platform due to the combined effect of reduced temperature and impact forces on the material and geometric properties of the structure. Thus, there is a need to understand the behaviour of offshore structures under impact forces in low-temperature conditions. Offshore Triceratops is one of the recent new-generation compliant platforms proved to be suitable for ultra-deepwater applications. The main aim of this study is to assess the response of triceratops under impact forces in Arctic environment numerically. As the buoyant legs of triceratops are susceptible to impact forces arising from ship platform collision, the numerical model of a buoyant leg is developed using Ansys explicit dynamics solver. The impact analyses is then carried out with rectangular box-shaped indenter representing the stem of a ship, under both ambient conditions and Arctic temperature (− 60 °C) and the local response of the platform is studied through force deformation curves and stress contours. In order to study the global response of the platform, the numerical model of triceratops is developed in Ansys Aqwa solver and analysed under the action of impact load time history obtained from explicit analysis of buoyant leg. The impact load on the buoyant leg resulted in the continuous periodic vibration of the platform. Furthermore, parametric studies were also carried out to investigate the effect of indenter velocity, size, and location on the impact response of triceratops under Arctic temperature, and the results are discussed.

Keywords Arctic · Buoyant leg · Cylindrical shell · Impact analysis · Triceratops

1 Introduction

In the recent past, oil production and drilling have been extended to the Arctic region in ultra-deep waters due to a reduction in ice-covered areas by global warming. The harsh cold environment poses several threats to the structural integrity and stability of the platform. Due to the continuous formation of ice sheets, the structures are continuously subjected to dynamic loading. In addition to wave, wind, and ice loads, the platforms may also undergo accidental loads arising due to ship platform collision. Along with the immense engineering challenges faced by the offshore structures from environmental and accidental loads in the Arctic region, the prevailing low temperature induces additional threats by affecting the performance of materials. The lowest temperature in the Arctic islands and continental regions during winter can be below − 60 °C. Structural steel used in the construction of offshore platforms suffers reduced toughness at low temperatures, which in turn affects the performance of the platform. Thus, the ice environment plays a major role in the design and operation of offshore platforms in the Arctic region.

Different types of offshore structures have been used for oil exploration and drillings, such as gravity-based structures, Tension Leg Platforms, and Spar platforms. However, the need for the innovative structural form remains unchanged due to the action of various environment and accidental loads on the offshore platforms constructed in hostile environment. The quest for the compatible design had paved the way for the development of new generation offshore compliant platforms such as buoyant legs, triceratops, and buoyant leg storage regasification platforms (Chandrasekaran and Nagavinothini 2018a, b). Offshore triceratops are one of the new generation offshore platform which is found to be highly suitable for the ultra-deep

✉ Srinivasan Chandrasekaran
drsekaran@iitm.ac.in

[1] Department of Ocean Engineering, IIT Madras, Chennai, Tamil Nadu, India

water applications. The main aim of this study is to assess the impact response of offshore triceratops in the Arctic environment. Offshore triceratops consists of three buoyant legs connected to the deck by ball joints. The buoyant legs are positively buoyant and are position restrained by a set of taut moored tethers. The ball joints restrain the transfer of rotational motion and allow only translational motion between the deck and buoyant legs, which reduces the response on the deck and provides comfortable working space. Preliminary investigations on triceratops at a water depth of 2400 m had shown that the structural geometry is adaptable to ultra-deepwater conditions in extreme sea states (Chandrasekaran and Nagavinothini 2017, 2018a, b, 2019; Srinivasan and Nagavinothini 2019; Nagavinothini and Chandrasekaran 2019). Hence, the impact analysis of triceratops is also attempted to assess the behavior of the structure in low temperature regions.

The buoyant legs are high;y susceptible ot the impact forces and these are normally designed as orthogonally stiffened cylindrical shells to withstand the hydrostatic pressure and lateral forces. Several studies reported the impact response of stiffened and unstiffened cylindrical shells and steel plated structures under different impact scenarios and blast loads (Mohammadzadeh and Noh 2015, 2017, 2019; Do et al. 2018; Cerik et al. 2015; Karroum et al. 2007). In addition to the assessment of local damage in structural elements due to impact forces, researchers have also attempted to investigate the global response of offshore platforms (Syngellakis and Balaji 1989; Storheim and Amdahl 2014; Amdahl and Edberg 1993). However, very few studies have been carried out to assess the impact response of structures at low temperature are. Kim et al. carried out an experimental and numerical investigation of steel plated structures in an Arctic environment. They also carried out a material tensile test to predict the mechanical properties of polar class high tensile steel of grade DH36 (Kim et al. 2016). Yan et al. also investigated the mechanical properties of normal strength mild steel and high strength steel S690 at different temperatures ranging from − 80 to + 30 °C and recommended design formulae (Yan et al. 2014). Park et al. investigated the crashworthiness characteristics of steel plated structures at low temperatures. They also suggested that the collision accidental limit state design should be carried out with low-temperature effect (Park et al. 2015). Paik et al. investigated the effect of low temperature on the quasi-static crushing of thin-walled steel structures under ship collisions in Arctic waters (Paik et al. 2011). DiPaolo et al. carried out experimental studies to investigate the effect of ambient temperature on a quasi-static axial-crush response of steel box components (DiPaolo and Tom 2009). The impact response analysis of new generation offshore triceratops have not been attempeted so far in the literature.

This paper presents the numerical analyses of stiffened cylindrical shell structure used as buoyant legs in triceratops under lateral impact forces using Ansys Explicit dynamics solver. The cylindrical shell is modeled using polar class high tensile steel of grade DH36 based on the material properties available in the literature. The damage profile and the force–deformation characteristics of the cylindrical shell are presented under different impact scenarios at normal temperature and Arctic temperature of − 60 °C. In addition, detailed parametric investigations was also carried out to assess the effect of impact velocity and indenter size on the response of triceratops under different temperatures. From the impact load time history obtained through explicit analysis, the time response analysis is then carried out using Ansys Aqwa to predict the global response of deck and buoyant legs under impact forces. The novelty of this study lies in the impact response analysis of one of the new generation offshore platforms which is in the developmental stage. As the impact response analyses under low temperature conditions are very rare in the literature, this study helps in understanding the complete behaviour of triceratops in Arctic region. In addition, the methodology adopted in the study to investigate the local and global response of triceratops can also be identified as a novel procedure which can be adapted to the analyses of other offshore platforms.

2 The Methodology of the Study

The risk of significant structural damage in a platform due to the impact load arising from ship platform collisions is far higher than that of environmental loads (Harding et al. 1983). According to standard regulations, offshore structures should be designed to withstand impact loads from 5000 tons vessel at a velocity of 2.0 m/s (DNV-RP-C204 2010b). Since the 1980s, the average size of the vessel has increased by about 100 tons, which increases the collision energy during accidents. It makes the average vessel to be capable of causing more damage to the platform (Kvitrud 2011). In this context, impact analysis is carried out in the current study by using a rectangular box-shaped indenter of length 10.0 m, breadth 5.0 m, and depth 2.0 m, representing the stem of a ship with 7500-ton displacement, which is located at 5.0 m above the Mean Sea Level. The indenter is considered to be perfectly rigid in the analysis, which confines the strain energy dissipation to cylindrical shell and stiffeners. The effect of impact velocity on the impact behavior of the

buoyant leg is investigated by varying it from 3.0 to 5.0 m/s, and the depth of indenter is varied from 1.0 to 3.0 m for parametric studies.

Initially impact analysis carried out on the buoyant leg modeled as orthogonally stiffened cylindrical shell using Ansys Explicit dynamics solver, in order to predict the deformation of the cylindrical shell and stiffeners. The impact load time history is developed from the numerical studies for an impact duration of 0.35 s. Followed by impact analysis, hydrodynamic time response analysis is carried out using Ansys Aqwa solver to predict the response of deck and buoyant legs. The methodology followed in the study is shown in Fig. 1. Triceratops being a multi-legged structure, all the three buoyant legs of triceratops are prone to accidental collisions. In this study, response analysis is carried out by applying impact force on buoyant leg one as shown in Fig. 2. The line of action of the indenter is along the positive x-axis of triceratops and assumed as the central impact on buoyant leg 1, as shown in Fig. 2.

3 Preliminary Design and Numerical Modeling

3.1 Triceratops

Triceratops is one of the new generation offshore compliant platforms developed by White et al. (2005). The triceratops geometry suitable for 2400 m water depth is developed based on the Perdido Spar platform in the Gulf of Mexico. The weight, height, buoyancy force, and the area of the deck are maintained the same as that of spar platform. The

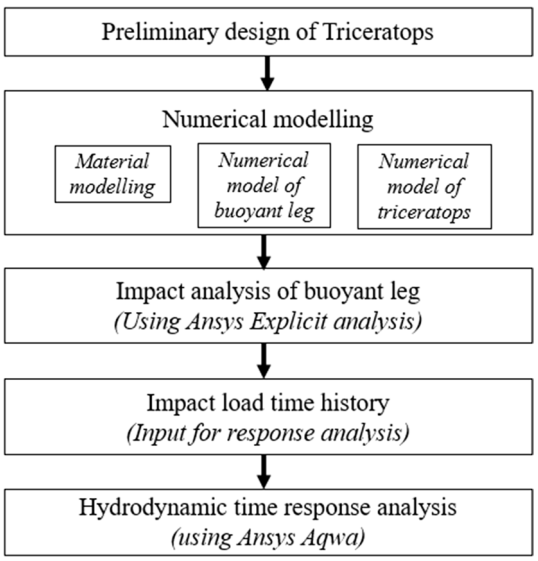

Fig. 1 Methodology of the present study

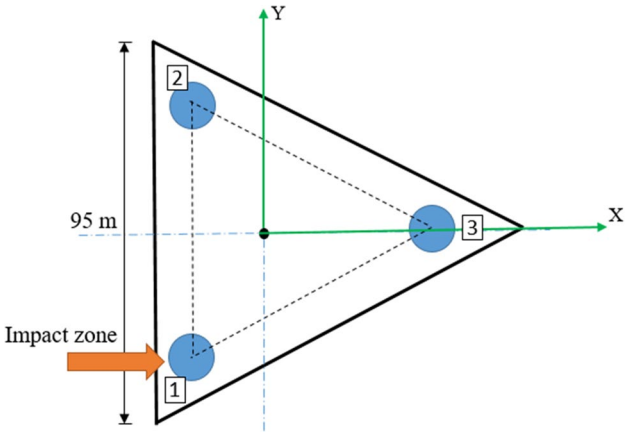

Fig. 2 Collision zone on buoyant leg 1

total buoyancy force is distributed to three buoyant legs. The shape of the deck is chosen as an equilateral triangle to enhance the symmetry. The geometric details of the triceratops are listed in Table 1. The topside is designed as an integrated truss deck system in such a way to provide sufficient space for the operation of the platform. The bending moment developed on each component in the deck is used for the preliminary design. The buoyant legs are deep draft cylindrical structures of 174.0 m height and 15.0 m diameter. The

Table 1 Details of triceratops (Chandrasekaran and Nagavinothini 2018a, b)

Description	Unit	Quantity
Water depth	m	2400
Unit weight of the material	kg/m^3	7850
Unit weight of sea water	kg/m^3	1025
Geometric details		
Diameter of Leg	m	15
c/c distance between the legs	m	62
Length of the buoyant leg	m	174
Freeboard	m	20
Draft	m	154
Tether length	m	2246
The vertical center of gravity of buoyant leg	m	− 113
Meta-centric height	m	36
Load details		
Self-weight + payload	MN	562
Buoyancy force	MN	821
Total tether force	MN	258
Other details		
Area of deck	m^2	3933
Area of tethers	m^2	2.356
Stiffness of tethers	GN/m	0.22

draft of the buoyant leg is about 89% of its total height. The hydrodynamic model of triceratops is developed by combining Ansys design modeler and Ansys Aqwa solver. The deck is modeled with three deck levels, and all the components in the deck are modeled using quadrilateral and solid triangular elements. The buoyant legs are modeled as tube elements or Morison elements and are connected to the deck by using ball joints. The buoyant legs are position restrained by a set of taut moored tethers, which are modeled as linear cables with initial pretension. The deck meshes with triangular and quadrilateral elements by program controlled optimum meshing. Mass, center of gravity and moment of inertia are separately defined for the deck and buoyant legs. The numerical model of triceratops is shown in Fig. 3a.

3.2 Buoyant Leg

The buoyant legs are designed as orthogonally stiffened cylindrical shell structures for intermediate environmental conditions in the Gulf of Mexico. The stiffeners are designed as per DNV standard regulations (DNV-RP-C202 2010a). The cylindrical shell is designed with ring frames at 3.0 m center to center distance and 70 numbers of stringers. The vertical stiffeners are designed as flat bars of 300×10 mm and are attached to the cylindrical shell internally. Explicit finite element methods are efficient in solving large deformation problems by advancing the solution of the problem in time using the current and previous velocities and coordinates of the system without solving global systems linear or nonlinear equations. Energy and linear momentum conservations are generally used in the explicit analysis to check the stability and accuracy of the solution (Benson 2017). The buoyant legs are separately modeled in Ansys design modeler and Ansys Explicit dynamics solver for impact analysis. The modeling is done using shell elements with hourglass damping and central difference time integration scheme. The rectangular box-shaped indenter is considered as the striking mass in this study, as shown in Fig. 3b, and it is assumed as perfectly rigid. The vertical lines in the cylindrical shell, as seen in the numerical model are stiffeners, and the horizontal lines are ring stiffeners or ring frames. Ring stiffeners near the indenter are named as R1, R2, and R3 for discussion. The time step is limited using the Courant–Friedrichs–Lewy condition, which ensures the stability and accuracy of the solution. Meshing is carried out using four-node quadrilateral shell elements. The quality of meshing is checked through momentum and energy conservation and hour-glassing during impact, and the mesh size of 0.3 m is found to be adequate. Viscosity coefficients are used to avoid discontinuities and damp the oscillations in the solution. The predominant component of deformation in impact analysis is the local indentation. In order to reduce

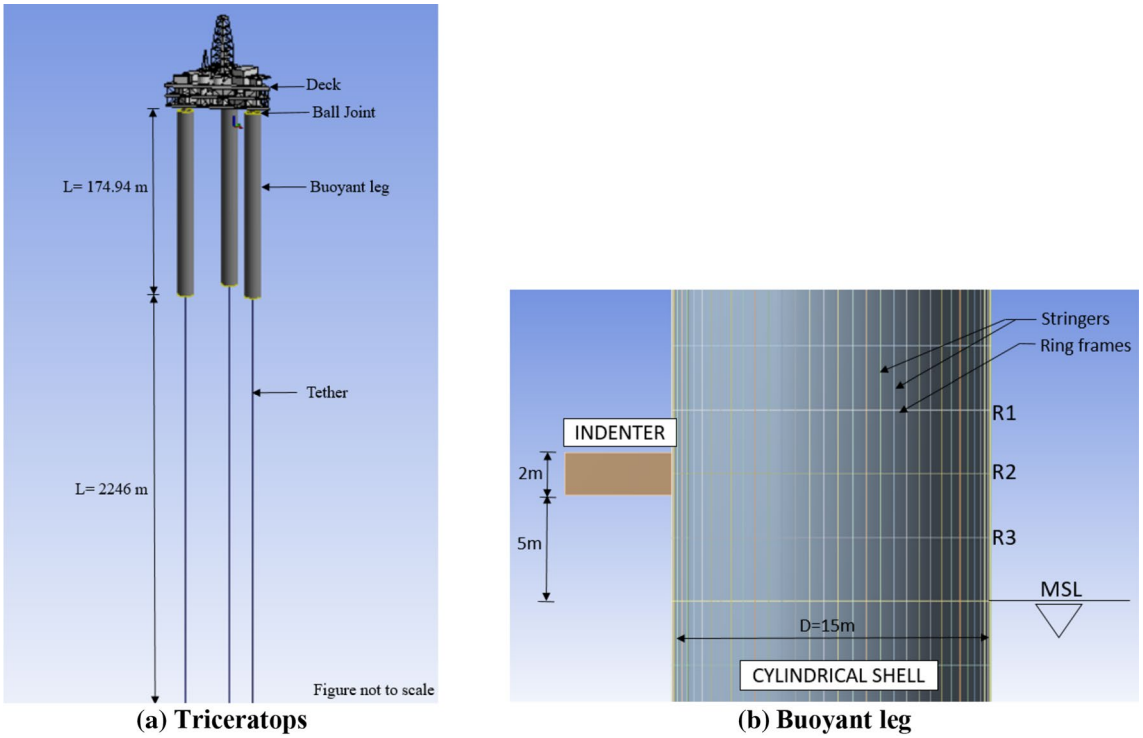

Fig. 3 Numerical model of triceratops

Table 2 Mechanical properties of DH36 steel at 0.001/s strain rate (Kim et al. 2016)

Temperature (°C)	Yield strength (N/mm^2)	Ultimate strength (N/mm^2)
Room temperature—RT	384	530
Arctic temperature (− 60 °C)—AT	446	607

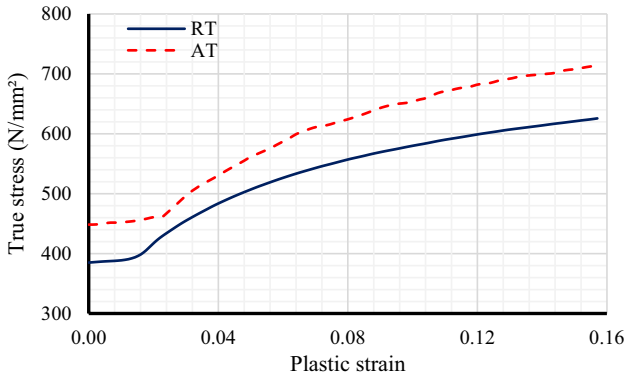

Fig. 4 True stress-plastic strain curves for DH36

the computational effort, the impact analysis is carried out only for the length of 45.26 m, shorter than the actual length of the buoyant leg. The ends of the buoyant leg in the developed model are considered as simply-supported. The striking mass is unrestrained only in the direction of impact.

4 Material Modelling

Low-temperature high strength steel materials should be capable of resisting various loads in extreme environmental conditions. The reduced temperature in the Arctic region affects the material properties significantly. At low temperature, tensile strength and yield strength of materials increases and toughness decrease. The decrease in tensile toughness significantly affects the performance of the structures (Kim et al. 2016). In this study, DH36 polar class high tensile steel is considered for developing the numerical model. Kim et al. determined the mechanical properties of DH36 steel at room temperature (RT) and Arctic temperature (− 60 °C) through quasi-static (0.5 mm/s) tensile tests. The mechanical properties and stress–strain curves developed by Kim et al. is used in this study for material modeling (Kim et al. 2016). The mechanical properties of DH36 steel at RT and − 60 °C at 0.001/s strain rate are listed in Table 2. It is evident that the yield strength increases with a decrease in temperature.

True stress–strain curves representing the basic plastic flow characteristics of the material at room temperature and an arctic temperature (− 60 °C) shown in Fig. 4 are used to define the material properties in order to predict the deformation characteristics. From the engineering stress–strain values, the true stress–strain curves are obtained by the following equations:

$$\sigma_t = \sigma_{eng}(1 + \varepsilon_{eng}) \tag{1}$$

$$\varepsilon_t = \ln(1 + \varepsilon_{eng}) \tag{2}$$

where σ_t is the True stress, σ_{eng} is the engineering stress, ε_t is the true strain and ε_{eng} is the engineering strain. The material is modeled in Ansys through multi-linear isotropic hardening model.

Followed by the numerical modelling of the buoyant leg and triceratops, numerical analyses are carried out to find the local and global response of the platform under impact force arising due to ship platform collision. The impact load time history obtained through the explicit analysis is applied as an external load on the buoyant leg to assess the total response of the structure.

5 Results and Discussions

5.1 Effect of Temperature

(a) Local response

In order to assess the impact behavior of the buoyant leg at different temperatures, impact analysis is carried out at room temperature and Arctic temperature at an impact velocity of 4.0 m/s for an impact duration of 0.35 s. The center of impact is at 6.0 m above the Mean Sea Level and 9.0 m below the top end of the buoyant leg. Based on the numerical analysis, it is found that the impact force causes local denting on the cylindrical shell which leads to flattening of the cross-section at the impact location and outward bulging of the shell at the ends of the flattened section. The deformation pattern of the buoyant leg is found to be similar under both temperature conditions, as shown in Fig. 5. From the longitudinal deformation pattern, it is observed that the indentation is not extended up to the upper end of the buoyant leg. The ring stiffener R2 at the impact location also gets flattened along with the deformation of the cylindrical shell and undergoes tripping, as shown in Fig. 6. The force–deformation curves at room temperature and Arctic temperature are shown in Fig. 7. The area under this curve gives the total energy absorbed by the buoyant leg. The flattening of

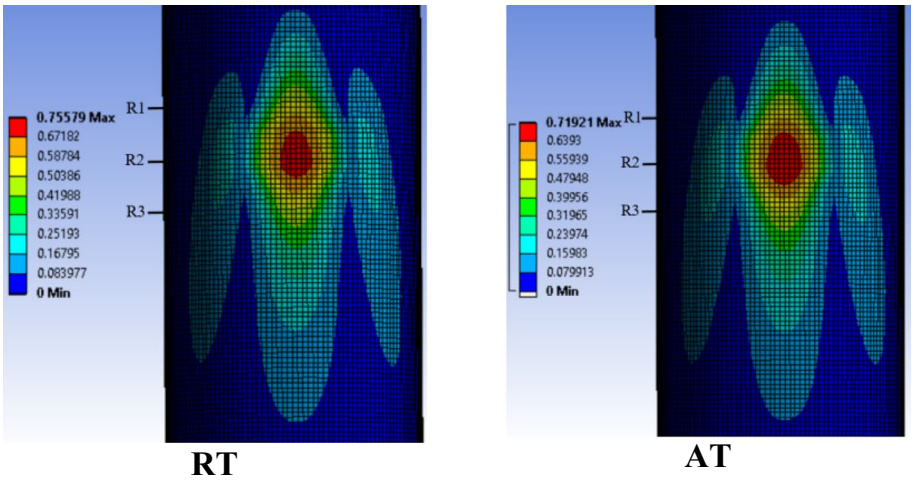

Fig. 5 Damage profile of the buoyant leg

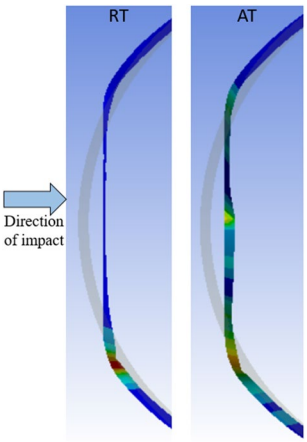

Fig. 6 Deformation of ring stiffener R2

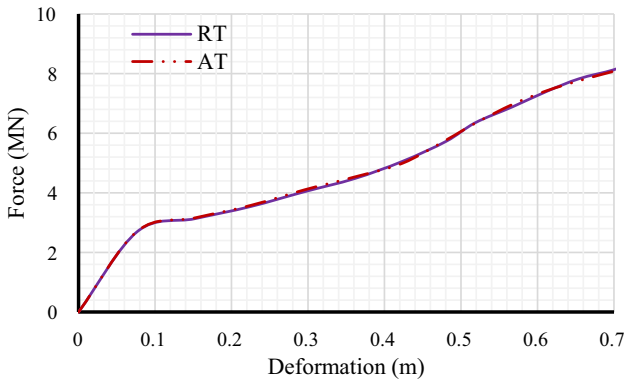

Fig. 7 Force deformation curve of the buoyant leg at different temperatures

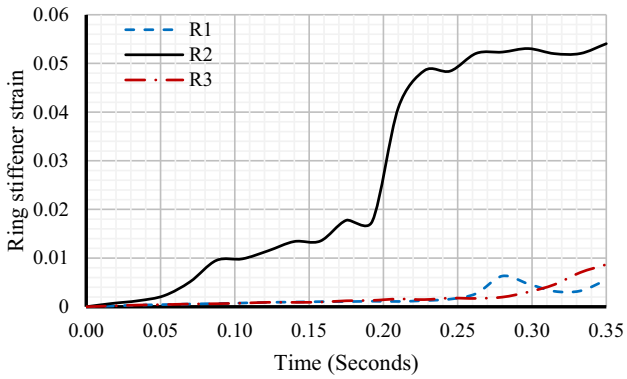

Fig. 8 Strain-time curve of ring stiffeners at an arctic temperature

the curve at 0.1 m indicates the tripping of stiffeners. Under both cases, the force–deformation curves are almost identical at initial stages showing good resistance to deformation and the peak impact force developed on the buoyant leg is about 8.81 MN and 8.79 MN at room temperature and arctic temperature, respectively.

At Arctic temperature, the maximum strain in ring stiffener R1 and R3 is found to be only 15% of ring stiffener R2 as seen from Fig. 8. The strain observed on the adjacent bays of impacted bay is within the elastic limit. It confirms that the ring stiffeners limit the spread of damage to the adjacent bays from impact location, and it acts as a hindrance to circumferential bending. Along with the deformation of the cylindrical shell, stringers also undergoes deformation. The stringers between the ring frames collapsed as a beam, and local tripping is observed in stringers close to the deformed ring stiffener. Though the impact occurs at the location of ring stiffener R2, maximum deformation along impact

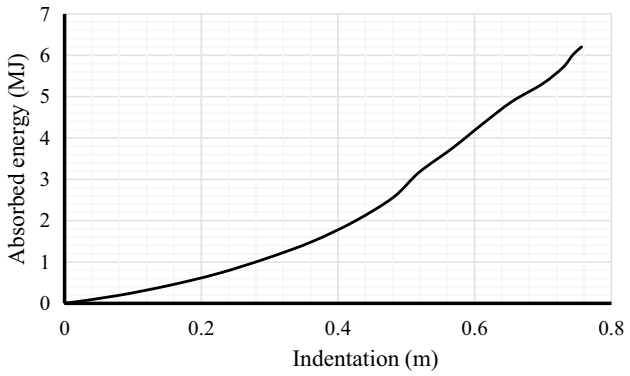

Fig. 9 Energy indentation curve of the buoyant leg at an arctic temperature

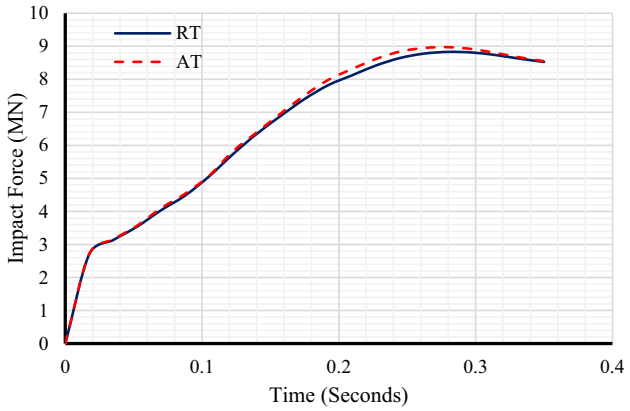

Fig. 10 Impact force time history under different temperatures

direction is observed only in the stringers. It should be noted that the presence of stiffeners increased the stiffness of the buoyant leg and its energy absorption capability. The energy indentation curve by the buoyant leg at Arctic temperature is shown in Fig. 9. The maximum energy absorbed by the buoyant leg is about 6.278 MJ.

(b) Global response

The impact load is applied as an external structure force on buoyant leg 1, and a hydrodynamic response analysis is carried out in Ansys Aqwa solver. The impact force time history under Room Temperature and Arctic Temperature is shown in Fig. 10. The results show that the impact load causes surge and pitch responses in triceratops; response in all other degrees of freedom are found to be negligible. The response of deck and buoyant leg one at different temperatures in the surge and pitch degrees of freedom are listed in Table 3. It can be seen that the response is also transferred to the other two buoyant legs through deck and ball joints. However, the responses in other buoyant legs are lesser than that of impacted buoyant leg. As the maximum peak force developed under different temperatures does not show significant variation, the response of deck and buoyant legs are also similar under both cases. Mean shift is not observed in the deck and buoyant legs under both temperature cases. As the impact load is acting above the Mean Sea Level, it induces considerable pitch response in buoyant legs. However, it is not transferred to the deck due to the presence of ball joints. The pitch response of the deck is only about 0.9% of pitch response in buoyant leg 1, which shows the effectiveness of ball joints. Despite the presence of ball joints which restrain the rotational motion between the deck and buoyant legs, a smaller pitch deck response is still observed in the deck due to the differential heave of buoyant legs. The responses in active degrees-of-freedom (surge and pitch) of the impacted buoyant leg at Arctic temperature are shown in Fig. 11. The response in surge and pitch degrees-of-freedom also induced tension variation in the tethers of all buoyant legs. However, the magnitude of responses in different degrees-of-freedom being considerably small under impact

Table 3 Response of triceratops under impact load on buoyant leg 1

Temperature	Degrees of freedom	Deck	Buoyant leg 1	Buoyant leg 2	Buoyant leg 3
RT	Surge (m)				
	Maximum	0.30	0.36	0.11	0.24
	Minimum	−0.29	−0.37	−0.10	−0.26
	Pitch (°)				
	Maximum	0.00	0.36	0.16	0.23
	Minimum	0.00	−0.34	−0.16	−0.21
AT	Surge (m)				
	Maximum	0.30	0.36	0.11	0.24
	Minimum	−0.29	−0.37	−0.10	−0.26
	Pitch (°)				
	Maximum	0.00	0.36	0.16	0.23
	Minimum	0.00	−0.34	−0.16	−0.21

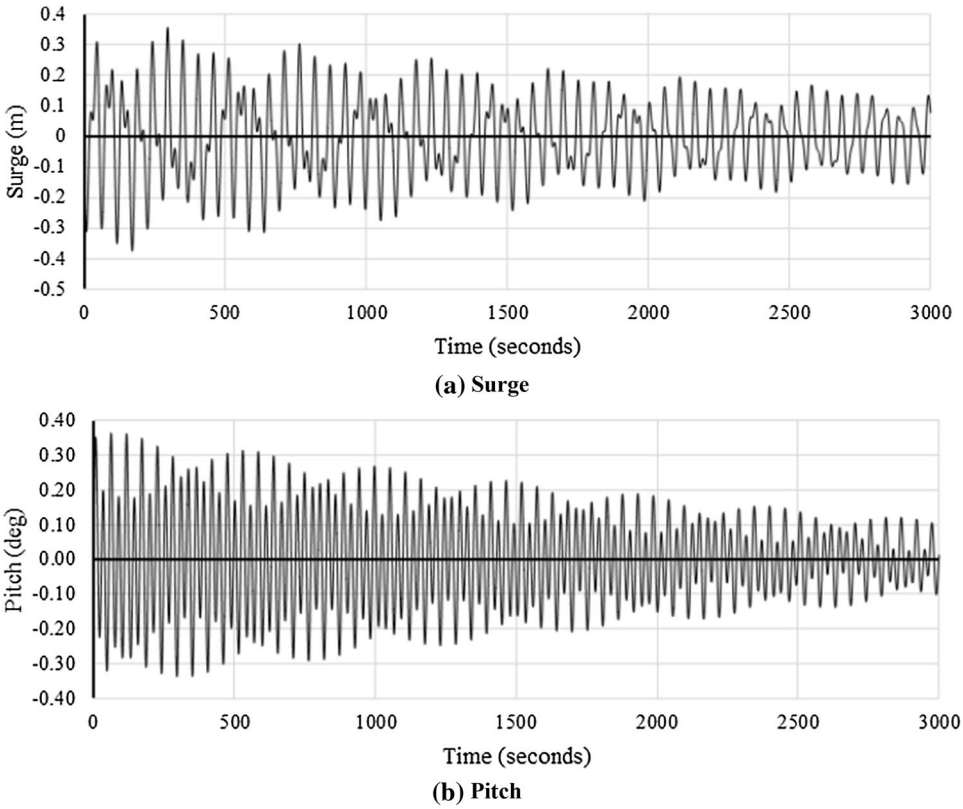

Fig. 11 Response of impacted buoyant leg at an arctic temperature

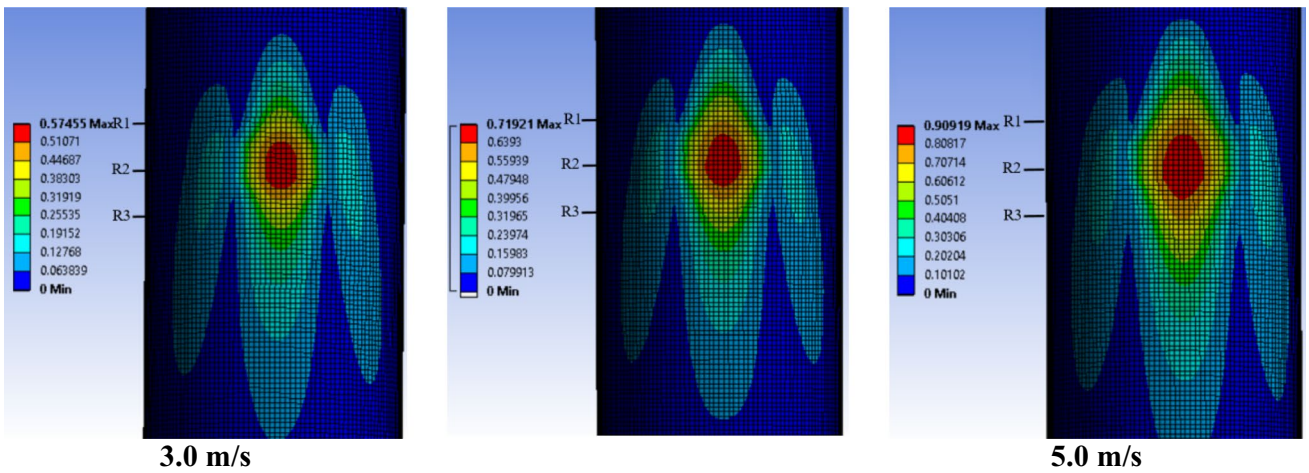

Fig. 12 Damage profile of buoyant leg at an arctic temperature under different impact velocities

load of short duration, the magnitude of tether tension variation observed in a triceratops is also very less. Maximum tether tension variation of 1.95% is only observed in the tethers in the impacted buoyant leg.

5.2 Effect of Indenter Velocity at Arctic Temperature

The indenter velocity is one of the important parameters that affect the total energy absorbed by the structure. The effect of impact velocity on the response of triceratops is assessed by varying the velocity from 3.0 to 5.0 m/s at Arctic

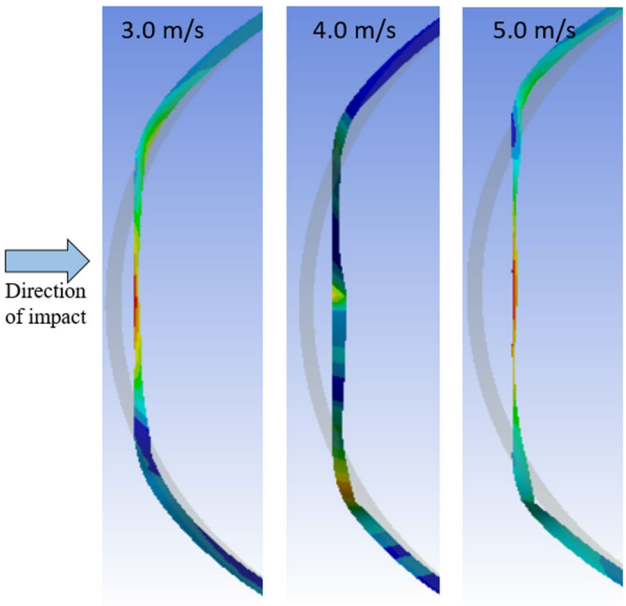

Fig. 13 Deformation of ring stiffener R2 at an arctic temperature under different impact velocities

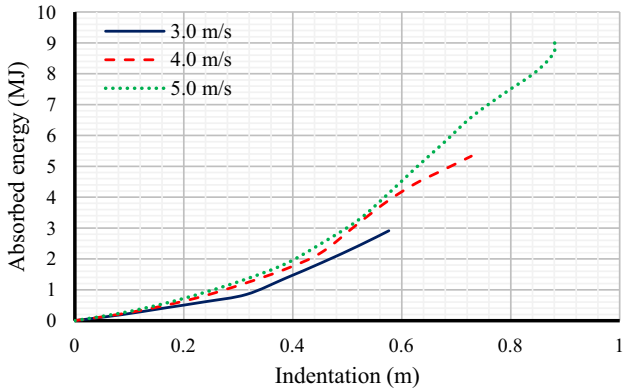

Fig. 14 Energy indentation curve of the buoyant leg at an arctic temperature under different impact velocities

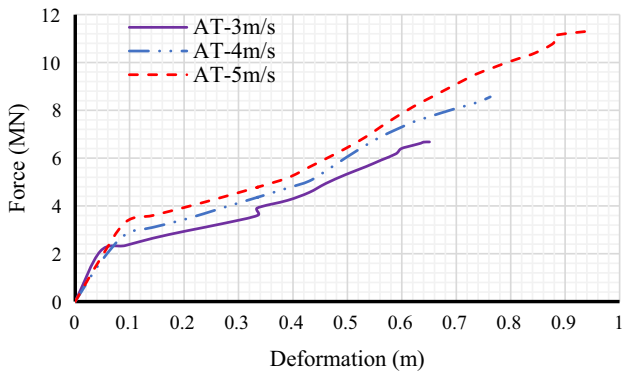

Fig. 15 Force deformation curve of the buoyant leg at different impact velocities

temperature. The size and weight of the rectangular indenter are maintained the same. As seen from the damage profile of the cylindrical shell in Fig. 12, the increase in impact velocity increases the area of contact between the indenter and buoyant leg, which in turn increases the deformation in the cylindrical shell and stiffeners. The deformation in the cylindrical shell increases from 0.58 m to 0.91 m with the increase in the impact velocity. The deformation of ring stiffener R2 shown in Fig. 13. Despite the increase in the contact area, the ring stiffeners hinder the spread of damage to adjacent bays from the impact zone, and the plastic strain is constrained in the bays close to the impact location. At low velocities, the impact force is resisted by stringer stiffeners, and maximum deformation is observed only in them. With the increase in the impact velocity, the ring and stringer stiffeners together resist the higher impact force by increasing stiffness of the cylindrical shell.

The energy indentation curve at different impact velocities is shown in Fig. 14. The energy absorbed by the buoyant leg increases forms 3–9 MJ with the increase in the impact velocity. The force–deformation curves at different impact velocities are shown in Fig. 15. The peak impact force acting on the buoyant leg increases from 6.7 to 11.5 MN with the increase in impact velocity. Every 1.0 m/s increase in the impact velocity increases the peak impact force by around 35%. At 5.0 m/s impact velocity, slope reduction of the force–deformation curves at both temperatures happens at two stages. At the first stage, the flattening of the curve occurs due to torsional buckling of stringer stiffeners. Then the slope increases due to the increase in the resistance to the impact force offered by the combined action of ring and stringer stiffeners. It shows the advantage of orthogonally stiffened cylindrical shells is in resisting the impact force at higher velocities.

The response of the deck and buoyant legs of triceratops in active degrees-of-freedom also found to be increasing with the increase in the impact velocity as seen from Table 4. With the increase in impact velocity by 1.0 m/s, surge response of deck increases by 30%. As the impact load acts on buoyant leg 1, it shows maximum responses under all cases. The tether tension variation of 2.3% and 1.9% are observed at impact velocities 3.0 m/s and 5.0 m/s respectively. Despite the increase in responses with the increase in impact velocity, tether tension variation is reduced due to a reduction in the mean shift of tension variation from the initial pretension. The surge and pitch response of the impacted buoyant leg at different impact velocities are shown in Fig. 16. Continuously decaying periodic oscillations are observed even at higher impact velocities but with the same period of vibration. Since the natural period of triceratops in surge degree of freedom is high due to its

Table 4 Response of triceratops under impact load on buoyant leg one at an arctic temperature

Impact velocity	Degrees of freedom	Deck	Buoyant leg 1	Buoyant leg 2	Buoyant leg 3
3.0 m/s	Surge (m)				
	Maximum	0.23	0.28	0.09	0.19
	Minimum	−0.22	−0.29	−0.09	−0.20
	Pitch (°)				
	Maximum	0.00	0.28	0.13	0.18
	Minimum	0.00	−0.26	−0.13	−0.17
5.0 m/s	Surge (m)				
	Maximum	0.39	0.45	0.12	0.30
	Minimum	−0.38	−0.48	−0.12	−0.33
	Pitch (°)				
	Maximum	0.01	0.47	0.18	0.30
	Minimum	0.00	−0.43	−0.18	−0.27

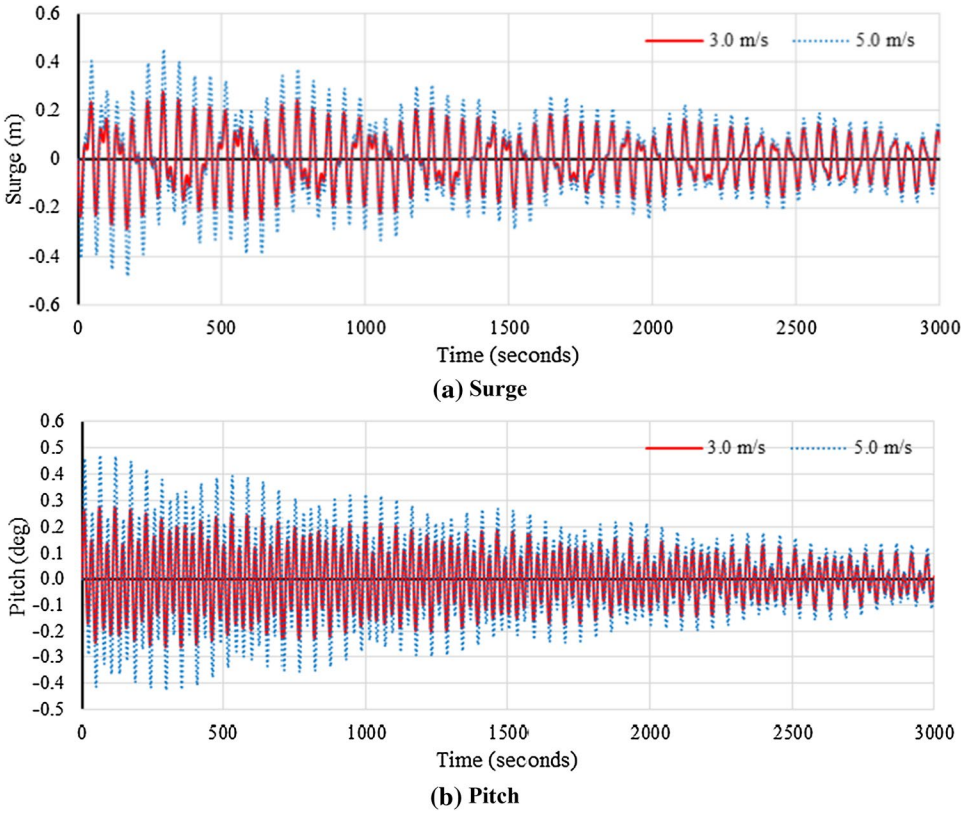

Fig. 16 Response of impacted buoyant leg at an arctic temperature under different impact velocities

compliance, the platform will undergo a large number of cycles about its original position.

5.3 Effect of Indenter Size at Arctic Temperature

The size of the indenter is also one of the important parameters that affect the behavior of structures under collisions. The impact analysis is carried out by changing the depth of rectangular indenter is varied from 1.0 to 3.0 m. The mass of the indenter is kept the same under all the cases. The numerical model of the buoyant leg and indenters of different depths are shown in Fig. 17. The different impact cases with varying indenter depths are represented by b/R ratio, where b is the depth of the indenter and R is the radius of the buoyant leg. The peak force developed during collision decreases with the increase in the b/R ratio from 11.9 to 7.8 MN at 0.35 s impact duration. The increase in depth of the indenter increases the contact area, which in turn results in increased deformation of the buoyant leg from 0.6 to 0.9 m.

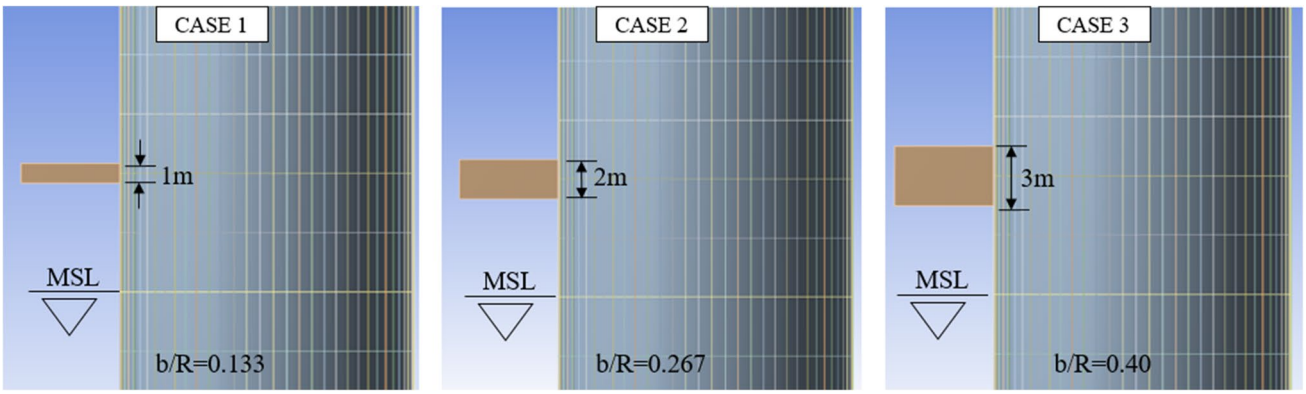

Fig. 17 Numerical model of different indenter sizes

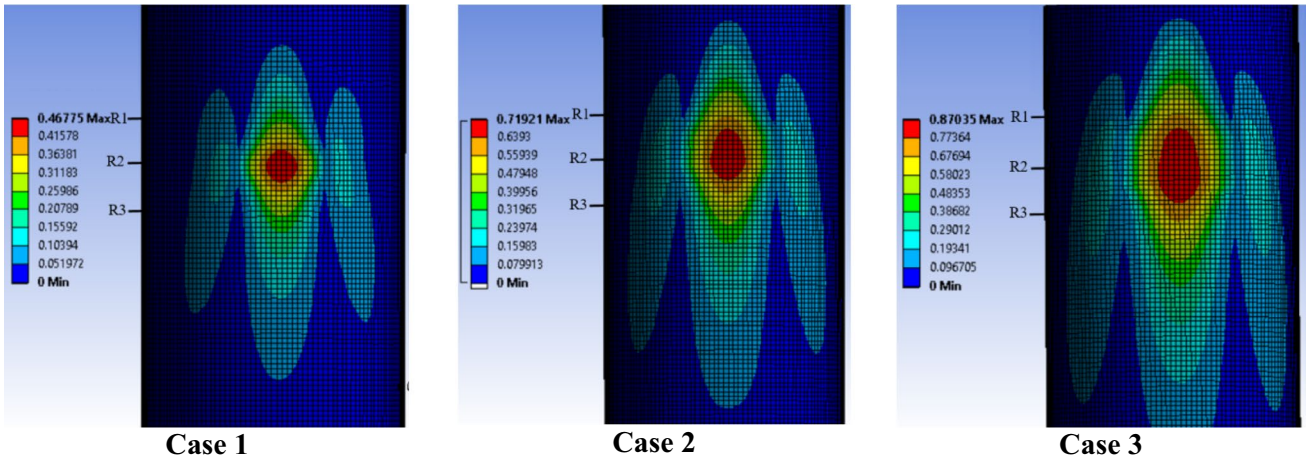

Fig. 18 Damage profile of buoyant leg at an arctic temperature under different indenter size

As seen from the damage profile of the cylindrical shell at various indenter sizes in Fig. 18, the increase in the size of the indenter increases the area of local indentation and plastic strain on the impact location. The extent of damage in circumferential and longitudinal direction also increases with the increase in b/R ratio. However, the pattern of damage in all cases is found to be similar. At lower indenter depths, maximum deformation is observed only in ring stiffener R2. However, with the increase in indenter depth, the ring stiffeners R1 and R3 also undergo deformation. The deformation of ring stiffener R2 is shown in Fig. 19. The absorbed energy-indentation curve of the buoyant leg under different cases are shown in Fig. 20. Maximum energy is attained at a shorter duration for lower b/R ratios.

The force–deformation curves under different cases are shown in Fig. 21. At lower b/R ratio, the slope of the force–deformation curve is high compared to the other two cases. The flattening of the curve is seen at b/R ratio of 0.133, which occurs due to the torsional buckling of stiffeners. The initial slope of the curve reduces with the increase in b/R ratio, which shows the increased deformation in the buoyant leg due to the higher contact area. Under higher b/R ratio, the buoyant leg undergoes increased deformation even at lower impact force. The results of the time response analysis of triceratops at Arctic temperature are listed in Table 5. Since the peak impact force is higher at lower b/R ratio, the surge and pitch response of deck and buoyant legs are higher. With the increase in the b/R ratio, the response of triceratops decreases. The surge and pitch responses of the impacted buoyant leg at Arctic temperature for various b/R ratios are shown in Fig. 22. Tether tension variation increases with the increase in b/R ratio from 1.95 to 2.33%.

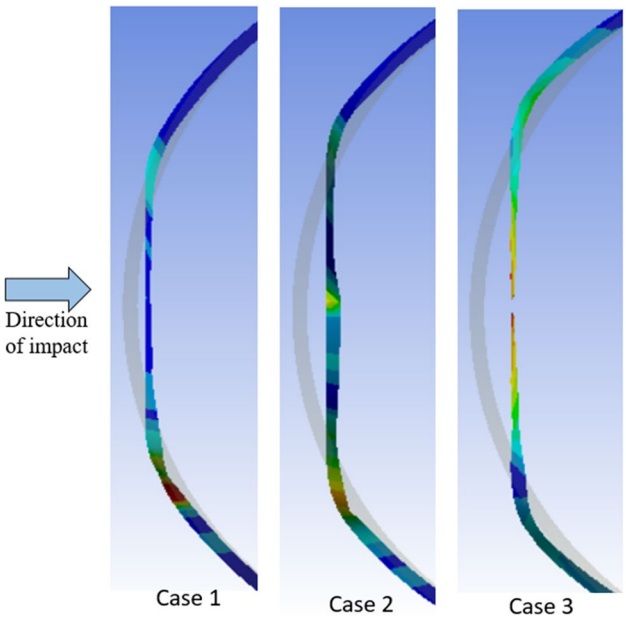

Fig. 19 Deformation of ring stiffener R2 at an arctic temperature under different indenter sizes

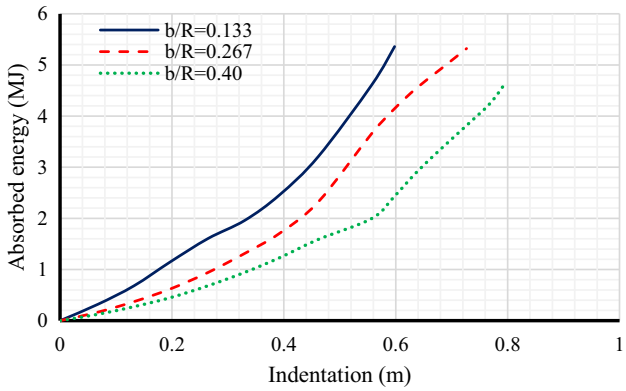

Fig. 20 Energy indentation curve of the buoyant leg at an arctic temperature under different indenter sizes

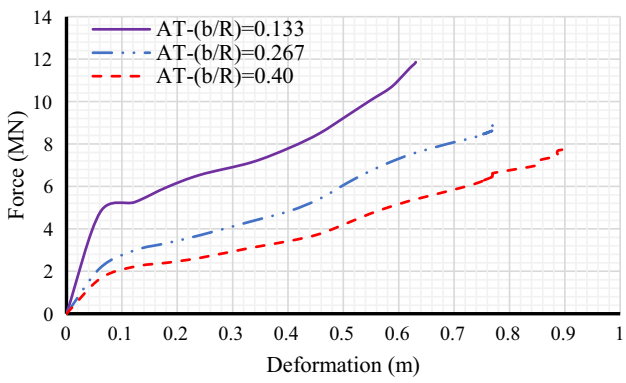

Fig. 21 Force deformation curve of the buoyant leg under different indenter sizes

5.4 Effect of Indenter Location at Arctic Temperature

The impact behavior and damage profile of the cylindrical shell also depend upon the location of the impact of the indenter on the buoyant leg. Hence, impact analysis carried out by varying the indenter location, as shown in Fig. 23. The center of impact of the rectangular indenter of 2.0 m depth is located at mid-bay between the ring stiffeners R2 and R3. The deformation of the buoyant leg due to a middle bay collision at an arctic temperature is shown in Fig. 24. The stringers play a major role in resisting the impact in mid-bay collision scenario, where it resists the impact load by acting as a beam and collapses due to the formation of a plastic hinge. Later, the ring stiffeners R2 and R3 undergoes deformation. The deformation of ring stiffener R2 is shown in Fig. 25. Due to the change in the circumferential strain and increased deformation of the cylindrical shell, the ring stiffener undergoes tilting. Both ring stiffeners R2 and R3 undergo highly concentrated strains at the ends of the flattened section.

The energy indentation curve of the buoyant leg under mid-bay collision at Arctic temperature is shown in Fig. 26. The energy absorbed by the buoyant leg is 5% lesser than that of the absorbed energy under impact location on ring stiffener R2. The force–deformation curve is shown in Fig. 27. In middle bay collision, stringers undergo maximum deformation compared to that of ring stiffeners. Stringers undergoes yielding followed by the ring frames. It is also evident from the flattening of the force–deformation curves at Arctic temperature. The plastic strain is constrained within the bay due to the presence of ring stiffeners. Under this colliding condition, ring stiffeners R2 and R3 undergoes almost equal deformation. The results of the time response analysis of triceratops for mid-bay collision are listed in Table 6. The significant response is observed only in surge and pitch degrees-of-freedom, and the response in all other degrees-of-freedom are found to be negligible. The surge and pitch response of the impacted buoyant leg are shown in Fig. 28. The tether tension variation under both cases is less than 3%.

6 Conclusions

The recent increase in the oil drilling and production in Arctic region necessitates a detailed investigation of innovation structural forms under such environmental conditions. The present study aims at investigating the response of a new generation offshore triceratops under impact forces arising due to ship platform collisons in ultra-deep waters. The local impact response of the buoyant leg of triceratops was studied through numerical analyses carried out using Ansys explicit dynamics solver. The impact load time history obtained from

Table 5 Response of triceratops under impact load on buoyant leg one at an arctic temperature

b/R ratio	Degrees of freedom	Deck	Buoyant leg 1	Buoyant leg 2	Buoyant leg 3
0.133	Surge (m)				
	Maximum	0.43	0.49	0.13	0.32
	Minimum	−0.41	−0.52	−0.13	−0.36
	Pitch (°)				
	Maximum	0.01	0.51	0.19	0.32
	Minimum	−0.01	−0.46	−0.19	−0.29
0.40	Surge (m)				
	Maximum	0.25	0.30	0.09	0.20
	Minimum	−0.25	−0.32	−0.09	−0.22
	Pitch (°)				
	Maximum	0.00	0.31	0.14	0.19
	Minimum	0.00	−0.29	−0.14	−0.18

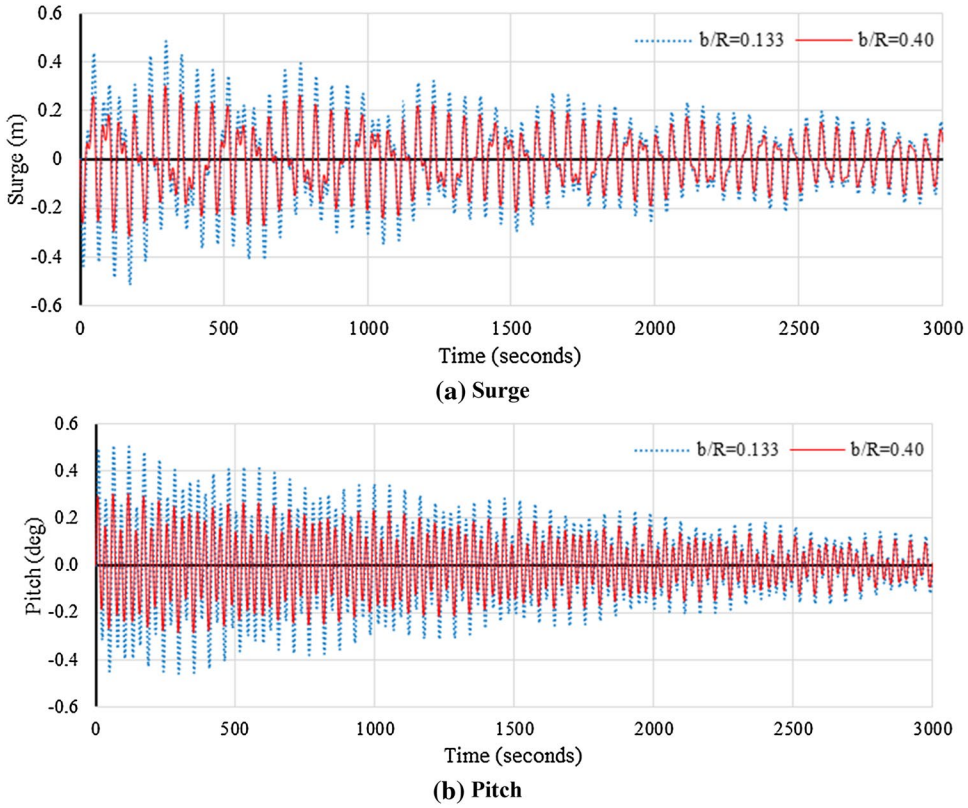

Fig. 22 Response of impacted buoyant leg at an arctic temperature under different indenter sizes

the explicit analyses was then applied as an external load on the buoyant leg of triceratops in Ansys Aqwa solver to assess the global response of the platform. In addition, parametric studies were also carried out by varying the impact velocity, indenter size, and impact location. Based on the numerical investigations carried out, the following conclusions were drawn:

- The impact causes a local dent on the buoyant leg, which leads to flattening of the cross-section at the impact loca-

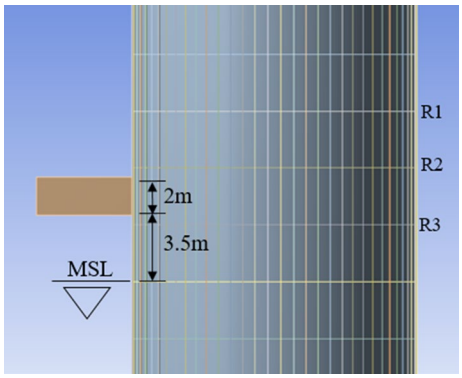

Fig. 23 Indenter location at mid-bay between ring stiffeners

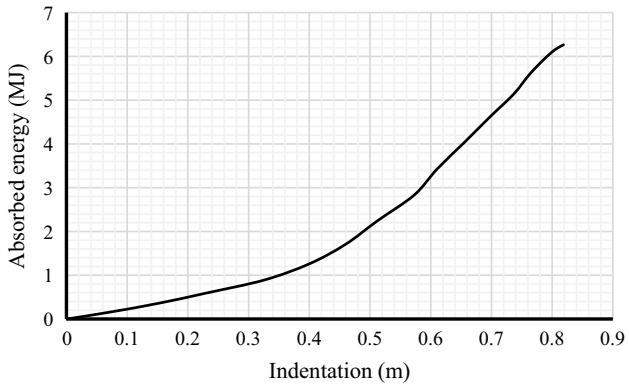

Fig. 26 Energy indentation curve of the buoyant leg at an arctic temperature under mid-bay collision

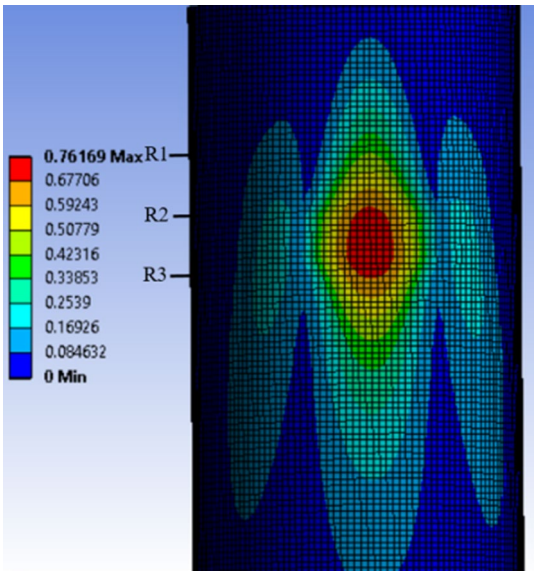

Fig. 24 Damage profile of buoyant leg during a mid-bay collision

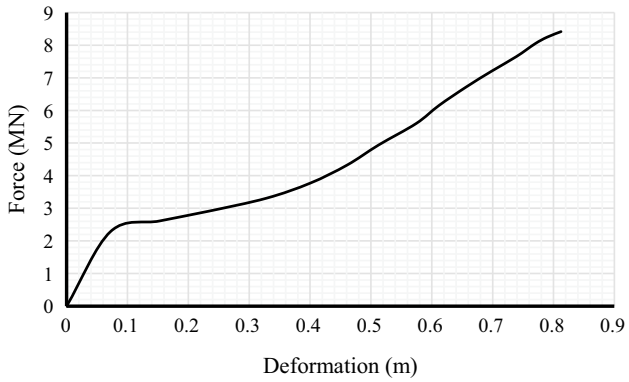

Fig. 27 Force deformation curve of the buoyant leg under mid-bay collision

Fig. 25 Deformation of ring stiffener R2 during a mid-bay collision

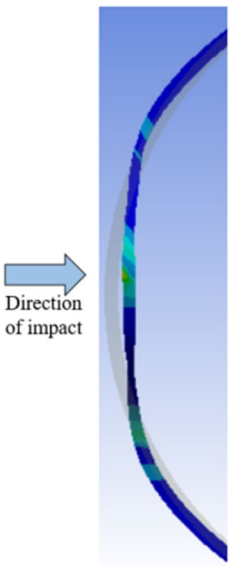

tion. The ring stiffeners hinder the spread of damage in the longitudinal direction. The ring frames and stringers increase the impact resistance of the buoyant leg by increasing its stiffness.

- The response of deck and triceratops depends on the maximum impact force and its rate of increase. The impact load produces continuously decaying surge and pitch responses under both room temperature and Arctic temperature. The change in the global response of triceratops due to the presence of ice in the Arctic environment is not considered in the study.
- The increase in the impact velocity increases the contact area and impact force on the buoyant leg. Impact velocity also affects the tether tension variation. The increase in

Table 6 Response of triceratops under impact load on buoyant leg one at mid-bay impact

Temperature	Degrees of freedom	Deck	Buoyant leg 1	Buoyant leg 2	Buoyant leg 3
AT	Surge (m)				
	Maximum	0.28	0.33	0.10	0.22
	Minimum	−0.27	−0.34	−0.10	−0.24
	Pitch (°)				
	Maximum	0.00	0.33	0.15	0.21
	Minimum	0.00	−0.31	−0.15	−0.20

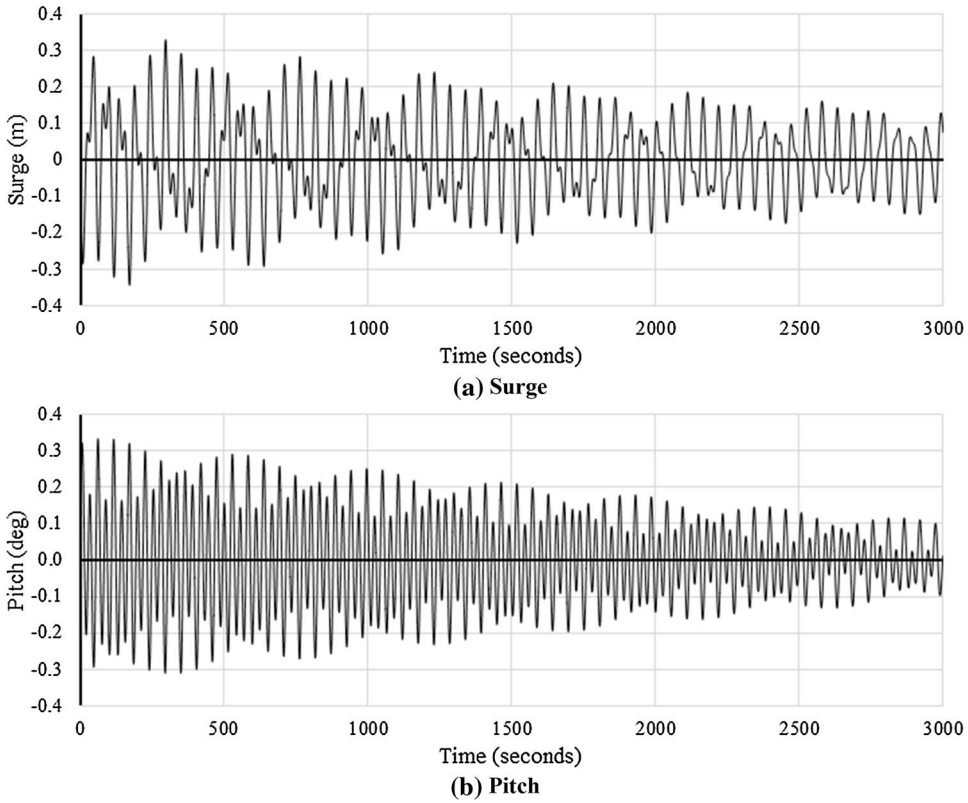

Fig. 28 Response of impacted buoyant leg at an arctic temperature under mid-bay collision

indenter size increases the contact area and plastic strain at the impact location.

- Under mid-bay collisions, maximum deformation is observed in the stringers, and the ring stiffeners constrain the plastic strain within the bay.
- Under all impact scenarios, the ball joints restrain the transfer the pitch motion from buoyant legs to the deck by about 99%, which shows the operational advantage of the platform even under accidental collisions.

This study helps in understanding in the complete response of the triceratops under different temperature conditions. As the triceratops are in the developmental stage, this study can be used as an aid in understanding the behaviour of triceratops under impact loads during the design of the platform.

References

Amdahl, J., & Edberg, E. (1993). Ship collision with offshore structures. In *Proceedings of the 2nd European conference on structural dynamics (EURODYN'93), Trondheim, Norway, June* (pp. 21–23).

Benson, D. J. (2017). Explicit finite element methods for large deformation problems in solid mechanics. In E. Stein, R. Borst, & T. J. Hughes (Eds.), *Encyclopedia of computational mechanics* (2nd ed.). Hoboken: Wiley.

Cerik, B. C., Shin, H. K., & Cho, S. R. (2015). On the resistance of steel ring-stiffened cylinders subjected to low-velocity mass impact. *International Journal of Impact Engineering, 84,* 108–123.

Chandrasekaran, S., & Nagavinothini, R. (2017). Analysis and design of offshore triceratops under ultra-deep waters. *World Academy of Science, Engineering and Technology, International Journal of Civil, Environmental, Structural, Construction and Architectural Engineering, 11*(11), 1520–1528.

Chandrasekaran, S., & Nagavinothini, R. (2018a). Tether analyses of offshore triceratops under the wind, wave, and current. *Marine Systems & Ocean Technology, 13*(1), 34–42.

Chandrasekaran, S., & Nagavinothini, R. (2018b). Dynamic analyses and preliminary design of offshore triceratops in ultra-deep waters. *Innovative Infrastructure Solutions, 3*(1), 16.

Chandrasekaran, S., & Nagavinothini, R. (2019). Tether analyses of offshore triceratops under ice force due to continuous crushing. *Innovative Infrastructure Solutions, 4*(1), 25.

DiPaolo, B. P., & Tom, J. G. (2009). Effects of ambient temperature on a quasi-static axial-crush configuration response of thin-wall, steel box components. *Thin-Walled Structures, 47*(8–9), 984–997.

Do, Q. T., Muttaqie, T., Shin, H. K., & Cho, S. R. (2018). Dynamic lateral mass impact on steel stringer-stiffened cylinders. *International Journal of Impact Engineering, 116,* 105–126.

Harding, J. E., Onoufriou, A., & Tsang, S. K. (1983). Collisions—What is the danger to offshore rigs? *Journal of Constructional Steel Research, 3*(2), 31–38.

Karroum, C. G., Reid, S. R., & Li, S. (2007). Indentation of ring-stiffened cylinders by wedge-shaped indenters—Part 1: An experimental and finite element investigation. *International Journal of Mechanical Sciences, 49*(1), 13–38.

Kim, K. J., Lee, J. H., Park, D. K., Jung, B. G., Han, X., & Paik, J. K. (2016). An experimental and numerical study on nonlinear impact responses of steel-plated structures in an Arctic environment. *International Journal of Impact Engineering, 93,* 99–115.

Kvitrud, A. (2011). Collisions between platforms and ships in Norway in the period 2001–2010. In *ASME 2011 30th International Conference on Ocean, Offshore and Arctic Engineering* (pp. 637–641). American Society of Mechanical Engineers. https://doi.org/10.1115/OMAE2011-49897.

Mohammadzadeh, B., & Noh, H. C. (2015). Numerical analysis of dynamic responses of the plate subjected to impulsive loads. *International Journal of Civil, Environmental, Structural, Construction and Architectural Engineering, 9*(9), 1194–1197.

Mohammadzadeh, B., & Noh, H. C. (2017). Analytical method to investigate nonlinear dynamic responses of sandwich plates with FGM faces resting on elastic foundation considering blast loads. *Composite Structures, 174,* 142–157.

Mohammadzadeh, B., & Noh, H. C. (2019). An analytical and numerical investigation on the dynamic responses of steel plates considering the blast loads. *International Journal of Steel Structures, 19*(2), 603–617.

Nagavinothini, R., & Chandrasekaran, S. (2019). Dynamic analyses of offshore triceratops in ultra-deep waters under wind, wave, and current. *Structures, 20,* 279–289.

Paik, J. K., Kim, B. J., Park, D. K., & Jang, B. S. (2011). On quasi-static crushing of thin-walled steel structures in cold temperature: Experimental and numerical studies. *International Journal of Impact Engineering, 38*(1), 13–28.

Park, D. K., Kim, D. K., Park, C. H., Park, D. H., Jang, B. S., Kim, B. J., et al. (2015). On the crashworthiness of steel-plated structures in an arctic environment: an experimental and numerical study. *Journal of Offshore Mechanics and Arctic Engineering, 137*(5), 051501.

Srinivasan, C., & Nagavinothini, R. (2019). Ice-induced response of offshore triceratops. *Ocean Engineering, 180,* 71–96.

Storheim, M., & Amdahl, J. (2014). Design of offshore structures against accidental ship collisions. *Marine Structures, 37,* 135–172.

Syngellakis, S., & Balaji, R. (1989). Tension leg platform response to impact forces. *Marine structures, 2*(2), 151–171.

Veritas, D. N. (2010a). Buckling strength of shells, recommended practice DNV-RP-C202. *Det. Nor. Ver. Class. AS, Veritasveien, 1*.

Veritas, D. N. (2010b). Design against accidental loads, recommended practice DNV-RP-C204.

White, C. N., Copple, R. W., & Capanoglu, C. (2005). Triceratops: An effective platform for developing oil and gas fields in deep and ultra-deepwater. In *The fifteenth international offshore and polar engineering conference*. Mountain View: International Society of Offshore and Polar Engineers.

Yan, J. B., Liew, J. R., Zhang, M. H., & Wang, J. Y. (2014). Mechanical properties of normal strength mild steel and high strength steel S690 in low temperature relevant to the Arctic environment. *Materials and Design, 61,* 150–159.